



**ARTICLE**

# Prediction and Optimization of the Thermal Properties of TiO<sub>2</sub>/Water Nanofluids in the Framework of a Machine Learning Approach

Jiachen Li<sup>1,2</sup>, Wenlong Deng<sup>3</sup>, Shan Qing<sup>1,2,\*</sup>, Yiqin Liu<sup>4</sup>, Hao Zhang<sup>1,2</sup> and Min Zheng<sup>1,2</sup>

<sup>1</sup>Sate Key Laboratory of Complex Nonferrous Clean Utilization, Kunming University of Science and Technology, Kunming, 650093, China

<sup>2</sup>Faculty of Metallurgical and Energy Engineering, Kunming University of Science and Technology, Kunming, 650093, China

<sup>3</sup>Jiangxi Guoxing Intelligent Energy Co., Ganzhou, 330300, China

<sup>4</sup>Faculty of Media and Information Engineering, Yunnan Open University, Kunming, 650500, China

\*Corresponding Author: Shan Qing. Email: m15087088903@163.com

Received: 24 October 2022 Accepted: 14 December 2022

## ABSTRACT

In this study, comparing multiple models of machine learning, a multiple linear regression (MLP), multilayer feed-forward artificial neural network (BP) model, and a radial-basis feed-forward artificial neural network (RBF-BP) model are selected for the optimization of the thermal properties of TiO<sub>2</sub>/water nanofluids. In particular, the least squares support vector machine (LS-SVM) method and radial basis support vector machine (RB-SVM) method are implemented. First, curve fitting is performed by means of multiple linear regression in order to obtain bivariate correlation functions for thermal conductivity and viscosity of the nanofluid. Then the aforementioned models are used for a predictive analysis of the dependence of its thermal conductivity and viscosity on temperature and volume fraction. The results show that the least squares support vector machine (LS-SVM) has a prediction accuracy higher than the other models. The model predicts the thermal conductivity of TiO<sub>2</sub>/water MSE =  $1.0853 \times 10^{-6}$ ,  $R^2 = 0.99864$ , MAE = 0.00092, RMSE = 0.00104, and the viscosity of TiO<sub>2</sub>/water MSE =  $8.1397 \times 10^{-6}$ ,  $R^2 = 0.99995$ , MAE = 0.00074, RMSE = 0.0009.

## KEYWORDS

Nanofluids; viscosity; thermal conductivity; machine learning; predictive modeling

## Nomenclature

ANN	Artificial neural network
MLR	Multiple linear regression
BP	Multilayer feedforward artificial neural network
RBF-BP	Radial basis feedforward artificial neural network
SVM	Support vector machines
RB-SVM	Radial basis support vector machine
LS-SVM	Least squares support vector machine
MSE	Mean square error
RMSE	Root mean square error
MAE	Mean absolute error



$R^2$	Regression coefficient
T	Temperature (°C)
$\varphi$	Volume fraction (vol%)
$x_i$	Related variables
$\omega^T$	Variable coefficient
x	Estimate
$x^s$	Actual value
c	Regularization parameter
$\sigma^2$	Nuclear parameter
$k_i^{exp}$	Experimental data
$k_i^{cal}$	Forecast data
Pa · s	Dynamic viscosity
W/(m·K)	Thermal conductivity

## 1 Introduction

Scholars and researchers have proposed several methods to improve the heat transfer of fluids [1–4]. One method proposed is to use fluids with better heat transfer properties. Nanomaterials have promising applications in different engineering fields. Incorporating nanomaterials into fluids, thus preparing nanofluids, was proposed [5–7]. Nanofluids are relatively new-generation fluids with better thermal properties than conventional fluids [8–10]. These fluids consist of a primary fluid and particles of 1–100 nm in size. Nanofluids, suspensions, or colloids consist of particles much smaller than 100 nm, which increase the total heat transfer coefficient between the These fluids consist of a primary fluid and particles of 1–100 nm in size. And the surrounding surface. This phenomenon gives nanofluids higher thermal conductivity than the base fluid [11–14]. Additionally, nanofluids can decrease operating costs, improve energy efficiency, and create a cleaner environment. The effects of different nanoparticle types and parameters (e.g., temperature, volume fraction, particle shape, and particle size) on nanofluids' thermal conductivity and viscosity have been studied and discussed in many articles [15–23].

Forecasting is a method of predicting the future based on existing information. In recent decades, artificial intelligence has advanced with the times due to the rapid development of computers. Machine learning has been widely used in engineering research, especially in predicting systems with nonlinear behavior. Several artificial intelligence-based model prediction methods exist, including artificial neural networks (ANN) [24], genetic algorithms (GA), pion swarm optimization (PSO), response surface methodologic (RSM) [25,26], support vector machine (SVM), and other swarm optimization methods to process data [27–29]. Artificial intelligence, as a trusted algorithm at this stage, is also used to predict nanofluid behavior and reduce laboratory costs by building models to predict the behavior of nanofluids [30–33].

Moreover, the large amount of data generated by experimental studies are also challenging to model with conventional techniques. In a generalized scheme of model prediction, the relationship between control factors and response variables is established. Traditional analytical methods have poor predictive power and poor coupling ability. Artificial neural networks to predict the behavior of nanofluids predicting thermal conductivity and viscosity have been the subject of several studies [34–37]. The designed artificial neural networks can predict the behavior of nanofluids, but the details of the learning algorithm are not described in their studies.

Ahammed et al. [38] investigated the effect of volume concentration and temperature on graphene-water nanofluids' viscosity and surface tension. Harandi et al. [39] investigated how temperature and volume fraction affected the thermal conductivity of EG/multi-walled carbon nanotube iron oxide liquids.

Measure the data at 0–2.3 vol% and  $T = 25^{\circ}\text{C}–50^{\circ}\text{C}$ . According to the predicted results, the thermal conductivity increased by 50% in most cases compared to the base fluid. Toghraie et al. [40] investigated the effect of nanoparticle volume fraction and temperature on the thermal conductivity of ZnO/EG nanofluids.  $T = 25^{\circ}\text{C}–50^{\circ}\text{C}$  and volume fraction of 0.1%–3.5% experiments showed that the thermal conductivity increased with increasing volume fraction and temperature. Also, high-temperature thermal conductivity was higher than low-temperature thermal conductivity. Soylu et al. [41] studied the influence of the doping rate of Ag/Cu doped  $\text{TiO}_2$  nanofluid on thermal properties. As the doping rates and concentrations of different materials were investigated in the temperature range of  $T = 40^{\circ}\text{C}–60^{\circ}\text{C}$ , the thermal conductivity increased with increasing doping levels. Alirezaei et al. [42] investigated the rheological behavior of MWCNT-MgO (10%–90%) hybrid nanofluid (oil-based) at different volume fractions, temperatures, and shear rates. The results showed that the dynamic viscosity of the nanofluid decreased with increasing temperature.

In some studies, researchers have used artificial neural network methods and described the details of the algorithms. Sharma et al. [43] studied the progress of machine learning in nanofluids and the advantages and disadvantages of various machine learning. This review mainly introduces the factors affecting the thermophysical properties of nanofluids, the application scenarios of nanofluids, and the application of various machine learning methods in predicting the properties of nanofluids. Esfahani et al. [44] predicted the thermal conductivity of water/silver oxide nanofluids. They used a two-stage approach combining ultrasonic devices, magnetic mixing, and acidity control methods to prepare water/silver oxide nanofluid. They examined the thermal conductivity of the nanofluid at a volume fraction of 0.125%–2% and  $T = 25^{\circ}\text{C}–50^{\circ}\text{C}$ . The results showed that increasing the volume fraction at higher temperatures significantly affected the increase in thermal conductivity due to the increase in Brownian motion caused by increasing temperature. Said et al. [45] studied the synthesis and stability of glycol-based ternary heterogeneous nanofluids, predicted the change in their viscosity under the influence of different volume fractions and temperatures using artificial neural networks, and determined the trend. Sharma et al. [46] studied the thermal properties of  $\text{Fe}_3\text{O}_4$ -MWCNT mixed nanofluids and established a model to predict the mixed nanofluids. Models using gene expression programming and adaptive neural fuzzy inference systems (ANFIS) were used to predict  $\text{Fe}_3\text{O}_4$ -coated mixed nanofluids, and GEP and ANFIS predicted thermal properties well. Ariana et al. [47] investigated the thermal conductivity of  $\text{Al}_2\text{O}_3$  water-based nanofluids. They predicted thermal conductivity data for 285 nanofluids at 0.0013–0.1 vol%, particle size 8–283 nm, and  $T = 1^{\circ}\text{C}–138^{\circ}\text{C}$ . The results show that increasing the volume fraction, increasing the liquid temperature, and decreasing the nanoparticle size leads to an increase in temperature and heat transfer. Masoumi et al. [48] proposed a new model for calculating the effective viscosity of nanofluids and judged its accuracy. Kanti et al. [49] synthesized ionic liquid (IL) and dispersed  $\text{Al}_2\text{O}_3$  nanoparticles to study the effects of temperature and concentration on their stability, viscosity, and thermal conductivity. The experimental results show that when  $T = 30^{\circ}\text{C}–60^{\circ}\text{C}$  and concentration 0–10 wt%, the thermal conductivity increases with temperature, and the viscosity increases with temperature—evaluating the thermophysical properties of INFs using the gene expression programming (GEP) model. Kanti et al. [50–53] prepared fly ash-Copper nanofluids by a two-step method, designed five prediction models, and analyzed their accuracy in predicting viscosity and thermal conductivity. An artificial neural network model was used to predict graphene oxide  $\text{Al}_2\text{O}_3$ /water,  $\text{SiO}_2$ /water ethylene glycol (50:50), ZnO-Ag/water, and  $\text{Al}_2\text{O}_3$ /ethylene glycol nanofluids [54–57]. The articles propose a simple perceptron feedforward neural network model to predict the thermal conductivity of these nanofluids. The thermal conductivity increases with increasing volume fraction and temperature.

According to the above literature review, the majority of studies at present have high costs and little experimental data. Secondly, all machine learning methods are used to study the single thermal properties of a particular nanofluid. This method cannot compare the advantages of different machine learning

methods in predicting the thermal properties of nanofluid, and it may have a different excellent effect in predicting other thermal properties. With this in mind, this paper investigates the accuracy of different machine-learning models in predicting nanofluids' thermal conductivity and viscosity based on a small amount of data. The highlight of this study lies in designing various optimized machine learning methods to predict the two thermal properties and compare their effects. Secondly, the neural network selected in many studies can only be applied to predicting large data volumes. This study uses a small data volume model to predict nanofluids. This paper uses several machine learning models to predict the thermal conductivity and viscosity of  $\text{TiO}_2/\text{water}$  nanofluids with 0.25–2 vol%. In this study, the grid search algorithm and cross-validation are applied to the machine learning model selected in this paper. The model is optimized to ensure its high accuracy and wide application.

## 2 Selection of Nanofluid

The experimental preparation of  $\text{TiO}_2/\text{water}$  nanofluids in the laboratory was chosen as the material for study in the paper [58]. It shows that titanium dioxide ( $\text{TiO}_2$ ) has excellent optical and electronic properties, low cost, high photocatalytic activity, chemically stable lines, non-toxicity, antibacterial properties, UV protection, and environmental cleanliness. Moreover, the thermal conductivity of  $\text{TiO}_2/\text{water}$  nanofluid was increased by 22% compared to other essential fluids [59]. The  $\text{TiO}_2/\text{water}$  nanofluid was prepared by selecting spherical  $\text{TiO}_2$  with a diameter of 20 nm and using deionized water as the base fluid. Choose spherical  $\text{TiO}_2$  particles with a diameter of 20 nm, use deionized water as the base solution, and add  $\text{TiO}_2$  in different proportions. Then put the liquid into the ultrasonic cell and vibrate to ensure that the nanoparticles are fully dispersed in the base liquid to prepare  $\text{TiO}_2/\text{water}$  nanofluids. Forty sets of  $\text{TiO}_2/\text{water}$  nanofluid thermal conductivity and viscosity data are shown in Fig. 1. The data were divided into 80% as the training set and 20% as the test set. According to the data plots, it was found that the thermal conductivity of the nanofluid increased and viscosity decreased as the temperature increased; as the concentration of nanoparticles increased, the thermal conductivity and viscosity increased.

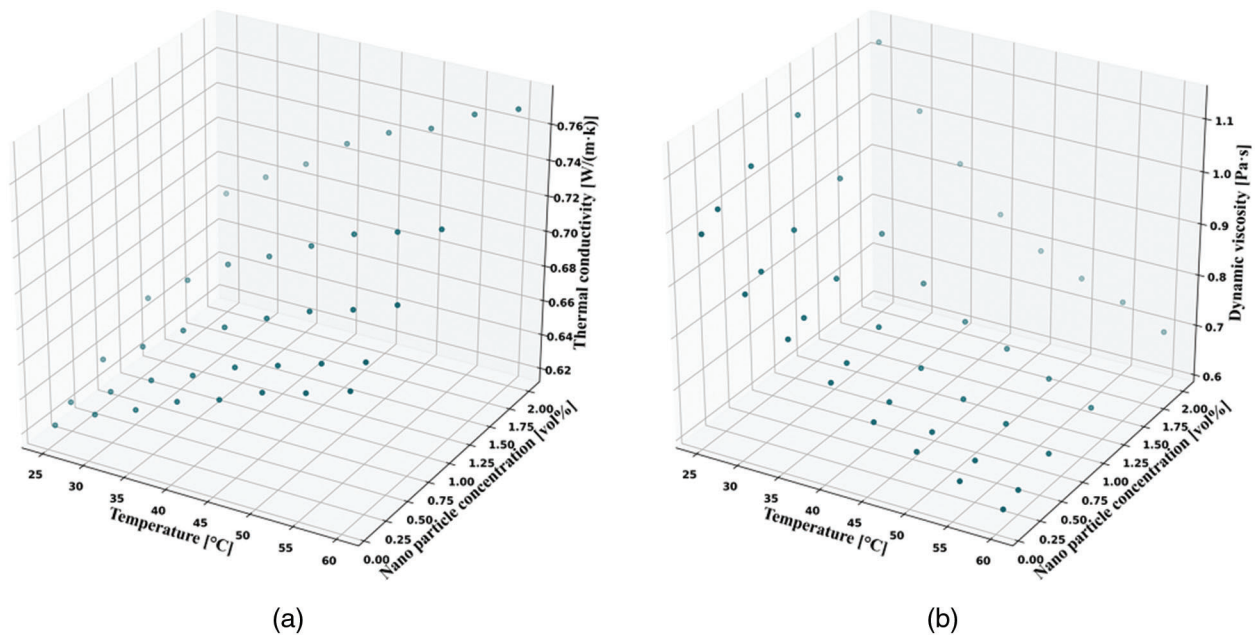


**Figure 1:** Thermal conductivity (a) and viscosity (b) data of  $\text{TiO}_2/\text{water}$  nanofluid

### 3 Research Methodology

In this section, we briefly introduce the selected machine learning models and the model accuracy evaluation criteria and highlight their advantages and disadvantages from a practical point of view. In this paper, we program the models using python and choose the most adaptable version 3.6. The sklearn library is called to write five machine-learning models and evaluation metrics, and the matplotlib library is used to plot the images.

#### 3.1 Machine Learning

Artificial intelligence-based multiple linear regression and artificial neural networks are models for testing a single nanofluid's thermal conductivity and viscosity. Therefore, in this paper, the most widely used multiple linear regression (MLR) model, the multilayer feedforward artificial neural network (BP) model, and the radial basis feedforward artificial neural network (RBF-BP) model of artificial neural networks are selected. Subsequently, two models, the Radial Basis Support Vector Machine (RB-SVM) and Least Squares Support Vector Machine (LS-SVM), which are more popular and have high accuracy at this stage, are developed.

##### 3.1.1 MLR Model

In real-world problems, changes in the dependent variable are often influenced by several important factors when it is necessary to use two or more influencing factors as independent variables to explain the changes in the dependent variable. If this relationship is linear, the linear multiple regression model can be used to describe it. The mathematical model of linear regression is Eq. (1).

$$f(\mathbf{x}_i) = \boldsymbol{\omega}^T \mathbf{x}_i + b \quad (1)$$

##### 3.1.2 BP Model

BP model is a kind of artificial neural network multilayer perceptron, which was proposed by a scientific group headed by Rumelhart and Hinton in 1986 [60]. BP neural networks can classify arbitrarily complex patterns and have excellent multi-dimensional function mapping. It can solve heterogeneous and other problems that simple perceptions cannot fight. Structurally, the BP model has three layers: an input layer, an implicit layer, and an output layer. In essence, it uses the grid error squared as the objective function and the gradient descent method to calculate the minimum value of the objective function. The primary process is as follows: first, the working signal is propagated forward, then the error signal is propagated backward to update the weights according to the error.

##### 3.1.3 RBF-BP Model

The BP neural network is improved by combining the BP neural network, which can better predict the unknown samples, and the RBF neural network, which can nonlinearly approximate any data set. RBF-BP composite neural network algorithm is a two-layer implicit layer neural network system. The RBF neural network is the first-level hidden layer, and the BP neural network is the second-level hidden layer.

##### 3.1.4 RB-SVM Model

Support vector machine is a supervised learning binary classification model that maps the feature vectors of the training set to some points in space, which the neural network classifies in an optimal line. Vapnik and Chervonenkis first proposed SVM in 1963, and the current version was modified by Hearst et al. [61]. RB-SVM uses kernel functions to replace the inner product, mapping the input data to higher space and thus solving for the best value. In this implementation, the radial basis function is utilized as the kernel function in the SVM, as shown in Eq. (2) [61].

$$K(\mathbf{x}, \mathbf{x}^s) = \exp\left(-\frac{\|\mathbf{x} - \mathbf{x}^s\|^2}{2\sigma^2}\right) \quad (2)$$

### 3.1.5 LS-SVM Model

The least squares support vector machine is a refinement and modification of the support vector machine that simplifies the solution process by solving a linear system of equations instead of the quadratic optimization problem in the SVM. The LS-SVM model consists of a regularization parameter ( $c$ ) and a kernel parameter ( $\sigma^2$ ). The kernel function defines the magnitude of the impact of a single training sample, with smaller values having a more significant impact and larger values having a minor impact.

### 3.2 Evaluation Metrics of Machine Learning Models

This study uses a total of four evaluation metrics, including mean square error (MSE), root means square error (RMSE), mean absolute error (MAE), and regression coefficient ( $R^2$ ), to evaluate the models [62–64]. Evaluation metrics are available to predict two nanofluids' thermal conductivity and viscosity and find the most accurate model. The MSE, RMSE, MAE, and  $R^2$  are mathematically by Eqs. (3) to (6) [62–64].

$$MSE = \sum_{i=1}^N \frac{(k_i^{exp} - k_i^{cal})^2}{N} \quad (3)$$

$$RMSE = \left\{ \sum_{i=1}^N \frac{(k_i^{exp} - k_i^{cal})^2}{N} \right\}^{0.5} \quad (4)$$

$$MAE = \sum_{i=1}^N \frac{|k_i^{exp} - k_i^{cal}|}{N} \quad (5)$$

$$R^2 = \frac{\sum_{i=1}^N (k_i^{exp} - \bar{\Delta k})^2 - \sum_{i=1}^N (k_i^{exp} - \Delta k_i^{cal})^2}{\sum_{i=1}^N (k_i^{exp} - \bar{\Delta k})^2} \quad (6)$$

where  $\bar{k}$  and  $N$  represent the average value of the thermal conductivity of the nanofluid and the number of experimental data on the thermal conductivity or viscosity of the nanofluid.

It is worth mentioning that when the MSE, RMSE, and MAE values converge to 0, and the model with  $R^2$  is close to 1, it is considered the most accurate model. The RMSE is mainly for outliers with large deviations, while the MAE is for all individual differences for the mean. In addition to these metrics, it is sometimes necessary to consider the model's size when searching for the best machine-learning model.

### 3.3 Grid Search CV

In machine learning models, hyperparameters are the parameters that must perform well. These include the number of neurons per layer and the number of hidden layers in the artificial neural network. If the hyperparameters are not selected correctly, the models will not perform well. Therefore, there are two ways to select hyperparameters: one is to fine-tune them empirically, and the other is to select different size parameters to bring into the model and pick the best ones. However, the above method requires manual debugging, which wastes much time and leads to failure to find the optimal hyperparameters. So cross-validation using grid search is the best method. The grid search is a parameter search. It is to adjust the parameters sequentially according to the set steps within the specified parameter range, train the model with the adjusted parameters, and compare the accuracy to find the best parameters.

### 3.4 Min-Max Normalized Data Set Preprocessing

Normalization refers to a linear variation of the initial data set, which results in a result mapped between 0 and 1. Data normalization speeds up gradient descent to find the optimal solution and improves accuracy using Eq. (7).

$$x_{\text{normal}} = \frac{x - x_{\text{Min}}}{x_{\text{Max}} - x_{\text{Min}}} \quad (7)$$

Data normalization where  $x_{\text{normal}}$  is the changed data value,  $x_{\text{Min}}$  and  $x_{\text{Max}}$  are the minima and maximum values of the sample data in the dataset.

## 4 Results and Discussion

This section summarizes and compares the machine learning models for the selected area. It compares the accuracy of various models with different parameters, selects the most accurate model from them, and analyzes the results.

### 4.1 Grid Search Cross-Validation to Select the Best Parameters

The evaluation metrics are filtered and validated by training and test set data using grid search CV to select the optimal number of neurons and parameters. All models are trained with 20 iterations and report only the best-selected model result, thus eliminating the effect of randomness on the performance of the developed models.

#### 4.1.1 MLR Model

Fig. 2 shows a roughly linear relationship between thermal conductivity and viscosity of TiO<sub>2</sub>/water, according to the MLR sub-correlation. Hence, the design of a one-time multiple linear regression model was more suitable for predicting the thermal conductivity model.

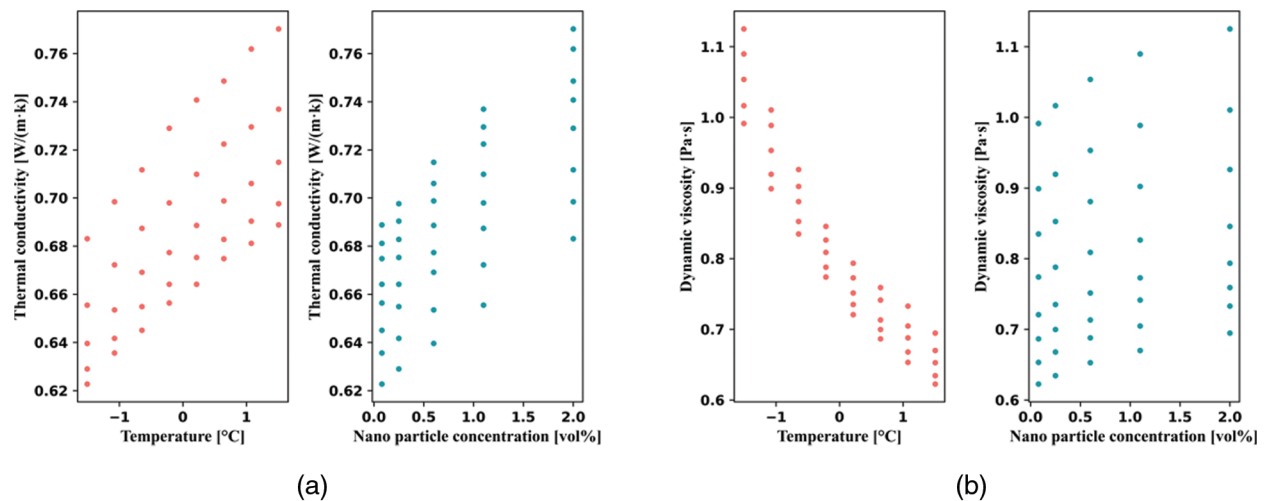


**Figure 2:** Correlation plot of MLR sub-analysis of thermal conductivity (a) and viscosity (b) of TiO<sub>2</sub>/water nanofluid

A curve-fitting model function Eq. (8) for the thermal conductivity of TiO<sub>2</sub>/water, a function of temperature and particle ratio, was fitted using a linear regression method. Eq. (9) is a linear relationship function of the viscosity of TiO<sub>2</sub>/water. T is the nanofluid temperature in °C and  $\varphi$  is the solid volume fraction in vol%. Table 1 also compares the training and test sets of the curves using accuracy metrics.

$$k_{nf} = 0.024965T + 0.037274\varphi + 0.657672 \quad (8)$$

$$k_{nf} = -0.128656T + 0.044632\varphi + 0.778602 \quad (9)$$

**Table 1:** Optimal parameters of the MLP model

TiO <sub>2</sub> prediction data	Database	Sensitivity accuracy analysis			
		MSE	R <sup>2</sup>	MAE	RMSE
Thermal conductivity	Train	1.7910 * e <sup>-5</sup>	0.98611	0.00332	0.00423
	Test	2.6231 * e <sup>-5</sup>	0.98611	0.00424	0.00512
Viscosity	Train	0.00089	0.95029	0.02536	0.02990
	Test	0.00098	0.94265	0.02639	0.03137

#### 4.1.2 BP Model

Fig. 3 shows the number of neurons in the BP neural network corresponding to the best MSE value according to grid search cross-validation. Based on the comprehensive comparison of multiple parameters (MSE, R<sup>2</sup>, MAE, RMSE) in Table 2. The TiO<sub>2</sub>/water thermal conductivity model is the most suitable model when the number of neurons in the hidden layer is up to 66. The TiO<sub>2</sub>/water viscosity model is the best model when the number of neurons in the hidden layer is up to 45. Fig. 4 shows the predicted data of the BP best-fit model compared with the actual data.

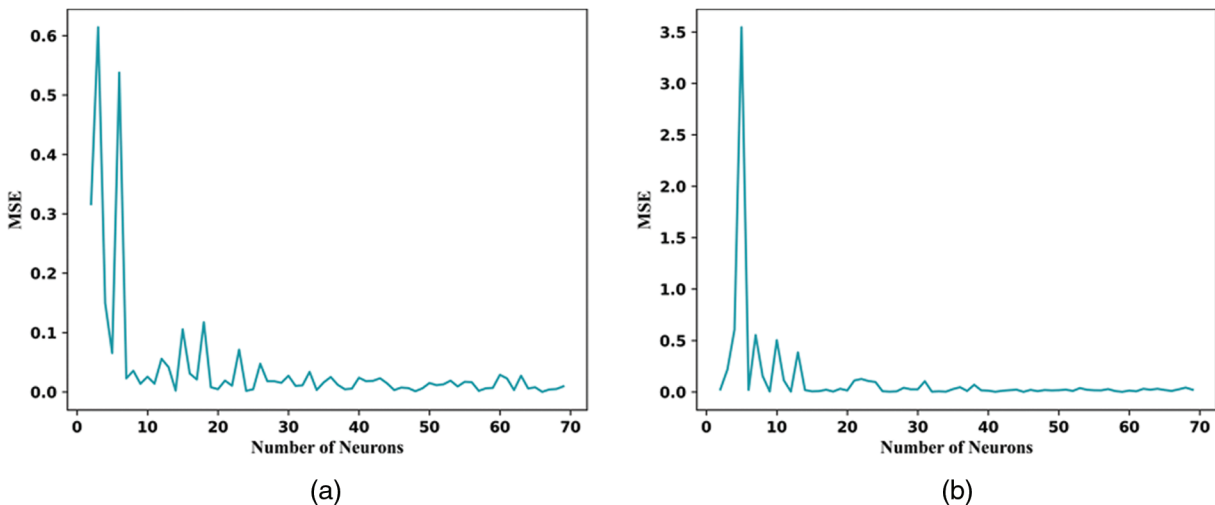


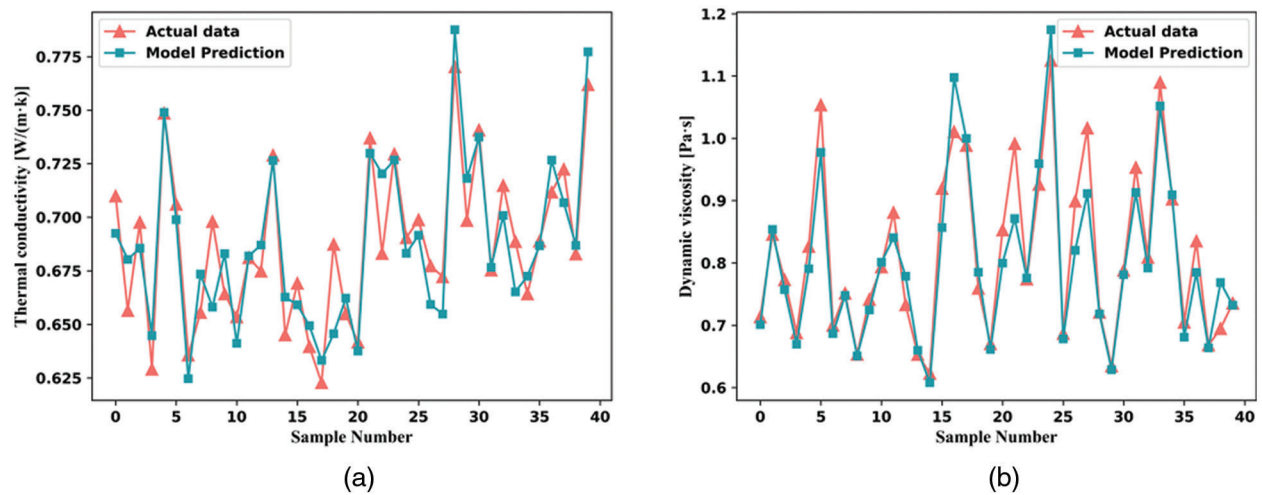
**Figure 3:** BP model MSE of thermal conductivity (a) and viscosity (b) of TiO<sub>2</sub>/water nanofluid vs. the number of hidden layer neurons

#### 4.1.3 RBF-BP Model

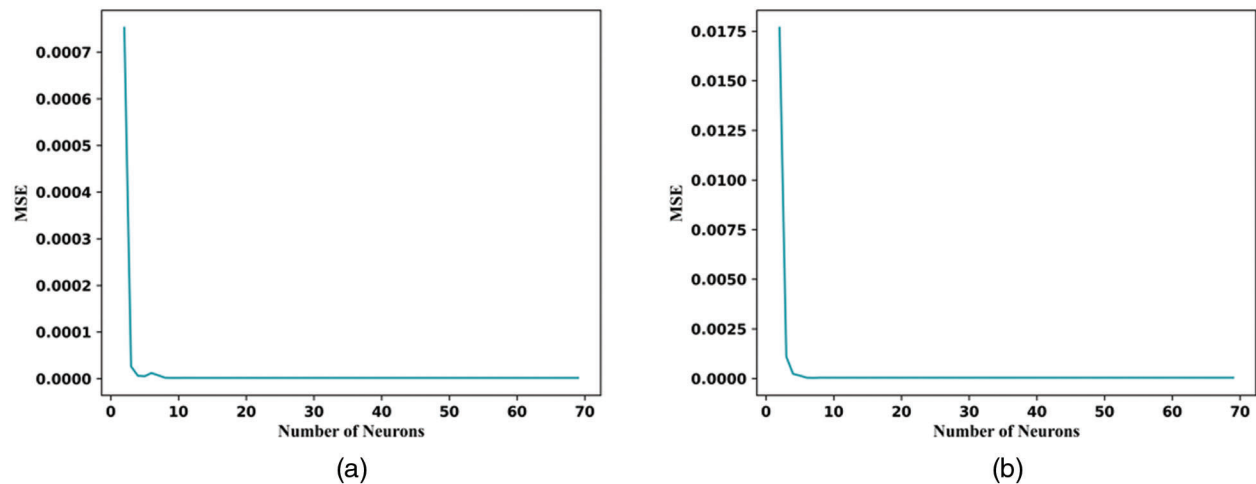
Based on the grid search CV, Fig. 5 shows the most suitable MSE model for selecting TiO<sub>2</sub>/water thermal conductivity and viscosity. Table 3 summarizes the results for the best parameters of the RBF-BP model. As can be seen, the RBF-BP model with 10 and 7 hidden neurons is the best model for this structure. Fig. 6 compares the predicted and actual data for the selected RBF-BP best model.

**Table 2:** Optimal parameters of the BP neural network model

TiO <sub>2</sub> prediction data	Optimal number of neurons	Database	Sensitivity accuracy analysis			
			MSE	R <sup>2</sup>	MAE	RMSE
Thermal conductivity	66	Train	0.00029	0.78030	0.01350	0.01707
		Test	0.00019	0.75829	0.01223	0.01387
Viscosity	45	Train	0.00202	0.88871	0.03186	0.04496
		Test	0.00130	0.92447	0.02721	0.03600



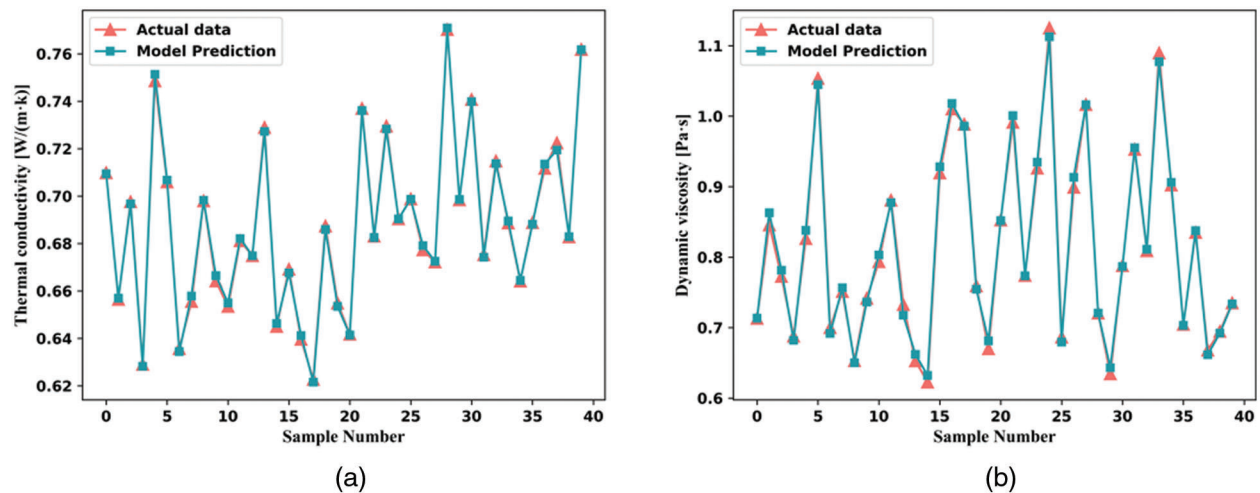
**Figure 4:** TiO<sub>2</sub>/water nanofluid thermal conductivity (a) and viscosity (b) BP model actual data vs. predicted data



**Figure 5:** MSE of TiO<sub>2</sub>/water nanofluid thermal conductivity (a) and viscosity (b) of RBF-BP model vs. number of hidden layer neurons

**Table 3:** Optimal parameters of RBF-BP neural network model

TiO <sub>2</sub> prediction data	Optimal number of neurons	Database	Sensitivity accuracy analysis			
			MSE	R <sup>2</sup>	MAE	RMSE
Thermal conductivity	10	Train	$1.5144 * e^{-6}$	0.99886	0.00102	0.00123
		Test	$1.7951 * e^{-6}$	0.9977	0.00099	0.00134
Viscosity	7	Train	$6.8713 * e^{-5}$	0.99622	0.00691	0.00829
		Test	$2.9337 * e^{-5}$	0.99829	0.00415	0.00542

**Figure 6:** Comparison of actual and predicted data from TiO<sub>2</sub>/water nanofluid thermal conductivity (a) and viscosity (b) RBF-BP models

#### 4.1.4 RB-SVM Model

The RB-SVM model selects the radial basis as the kernel function and the regularization parameter (c) according to the kernel function. Fig. 7 shows how the appropriate parameters are selected based on the MSE for each grid of  $\log_{10}-3$  to  $\log_{10}1$ . Table 4 shows the best parameters determined through a grid search. Fig. 8 compares the predicted and actual data of the appropriate model chosen for BP-SVM.

#### 4.1.5 LS-SVM Model

According to the model parameters  $\sigma^2 = 0.01 - 100$  and  $\sigma^2 = 1 - 10000$ , the kernel parameters are set at 3.24 and 1.91, and the evaluation index is found to be suitable. In this paper, set  $\sigma^2 = 3.24$  and use grid search CV to select the most appropriate regularization parameter kcp.

Fig. 9 shows the results of the selection of different regularization parameters, as well as judging the MSE values for the results obtained. Table 5 indicates that the LS-SVM model with  $c = 94.7322$  and  $c = 4155.4553$  has the best structural model parameters. Fig. 10 compares the selected LS-SVM best model prediction data with the actual data.

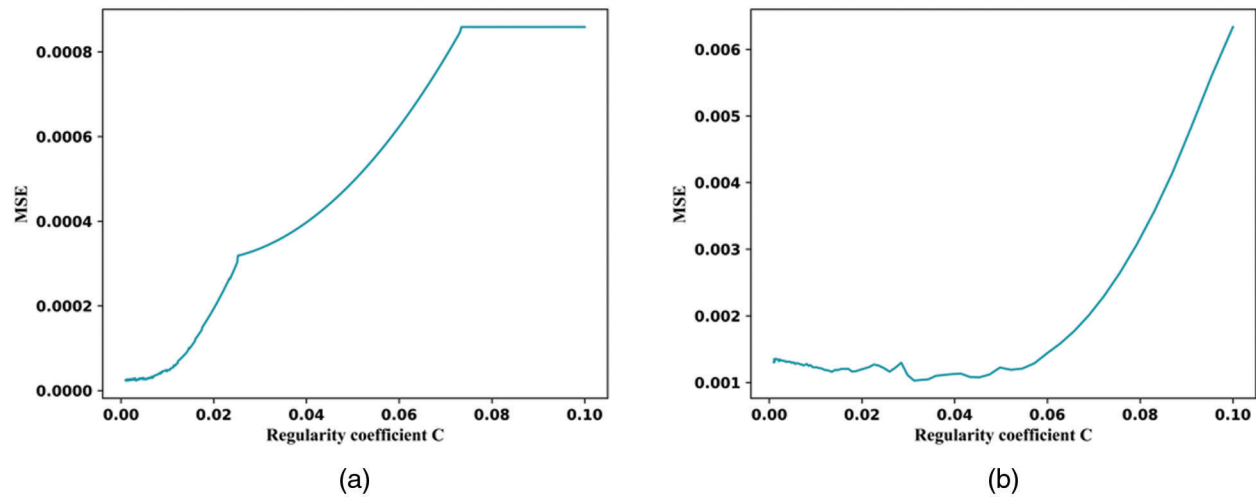


**Figure 7:** MSE of RB-SVM model for thermal conductivity (a) and viscosity (b) of TiO<sub>2</sub>/water nanofluid vs. regularized parameters

**Table 4:** Optimal parameters of RB-SVM model

TiO <sub>2</sub> prediction data	Regularization parameter	Database	Sensitivity accuracy analysis			
			MSE	R <sup>2</sup>	MAE	RMSE
Thermal conductivity	0.00138	Train	1.8737 * e <sup>-5</sup>	0.98587	0.00305	0.00433
		Test	2.3435 * e <sup>-5</sup>	0.97054	0.00388	0.00484
Viscosity	0.03126	Train	0.00088	0.95153	0.02544	0.02967
		Test	0.00103	0.94011	0.02627	0.03206

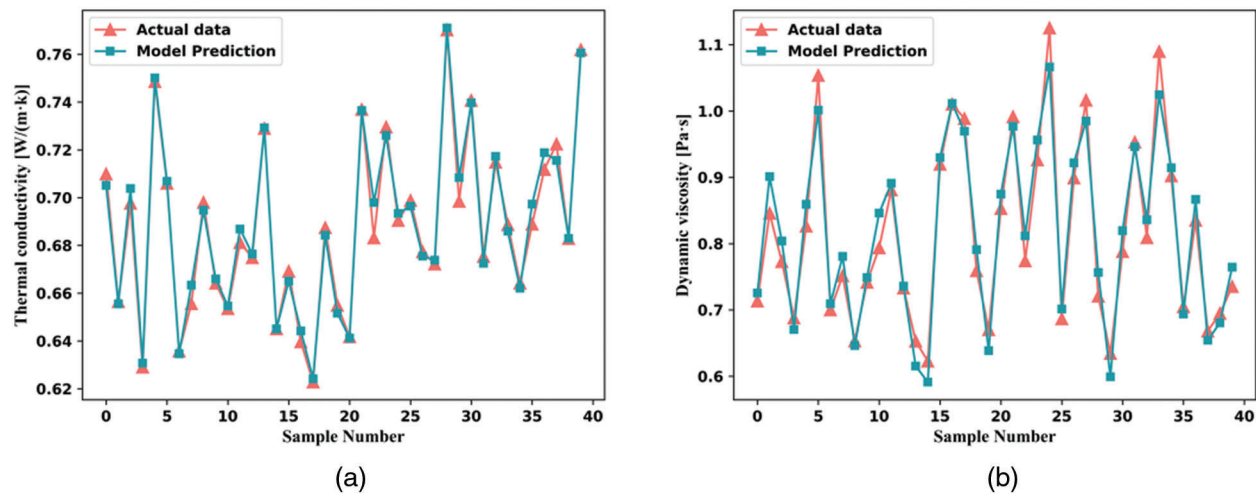


**Figure 8:** TiO<sub>2</sub>/water nanofluid thermal conductivity (a) and viscosity (b) RB-SVM model actual data vs. predicted data

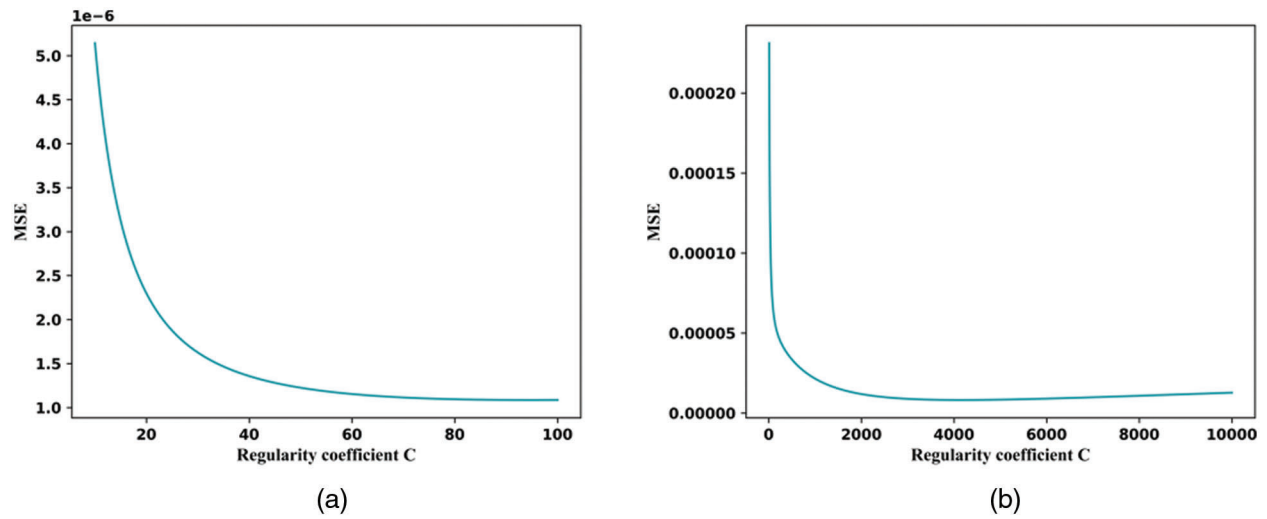


**Figure 9:** LS-SVM model MSE vs. regularized parameters for thermal conductivity (a) and viscosity (b) of TiO<sub>2</sub>/water nanofluid

**Table 5:** Optimal parameters of LS-SVM model

TiO <sub>2</sub> prediction data	Optimal nuclear parameter kcp	Optimal nuclear parameter	Database	Sensitivity accuracy analysis			
				MSE	R <sup>2</sup>	MAE	RMSE
Thermal conductivity	0.67615	94.7322	Train	2.0793 * e <sup>-6</sup>	0.99843	0.00108	0.00144
			Test	1.0853 * e <sup>-6</sup>	0.99864	0.00092	0.00104
Viscosity	0.86569	4155.4553	Train	5.1781 * e <sup>-6</sup>	0.99972	0.00182	0.00228
			Test	8.1397 * e <sup>-6</sup>	0.99952	0.00230	0.00285

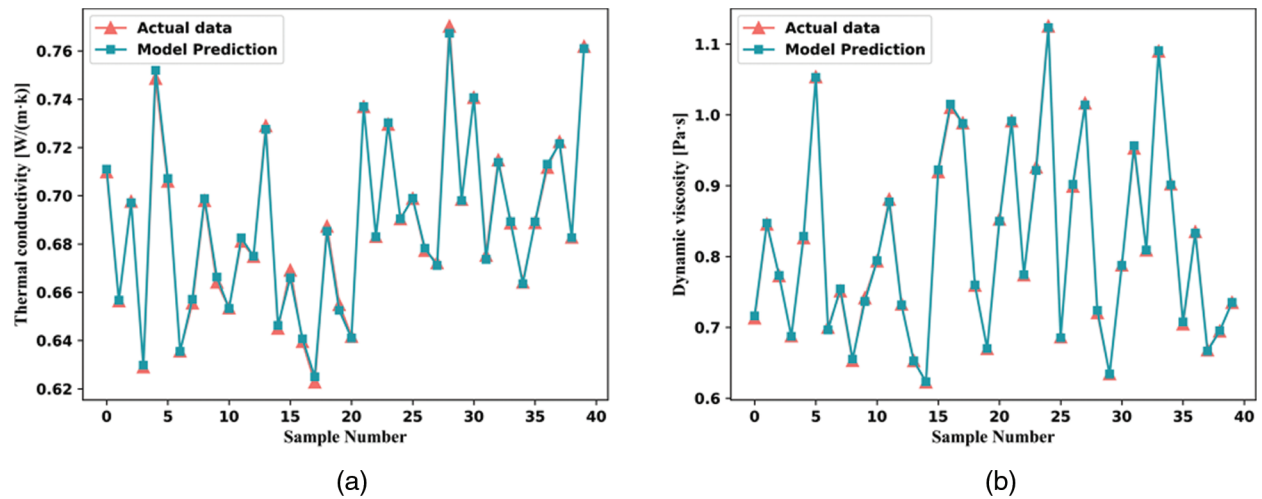


**Figure 10:** TiO<sub>2</sub>/water nanofluid thermal conductivity (a) and viscosity (b) LS-SVM model actual data vs. predicted data

#### 4.2 Finding the Best Model

This study aims to determine the most accurate model to predict the thermal conductivity of TiO<sub>2</sub> nanofluid using small data volumes and therefore compares the prediction accuracy of multiple models. The optimal parameter results for BP, RBF-BP, RB-SVM, and LS-SVM applied in this paper are reported in Table 6, along with their data results for MSE, R<sup>2</sup>, MAE, and RMSE.

**Table 6:** Comparison of optimal parameters of different machine learning

TiO <sub>2</sub> prediction data	Machine learning	Database	Sensitivity accuracy analysis				
			MSE	R <sup>2</sup>	MAE	RMSE	
Thermal conductivity	BP	Train	0.00029	0.78030	0.01350	0.01707	
		Test	0.00019	0.75829	0.01223	0.01387	
	RBF-BP	Train	1.5144 * e <sup>-6</sup>	0.99886	0.00102	0.00123	
		Test	1.7951 * e <sup>-6</sup>	0.9977	0.00099	0.00134	
	RB-SVM	Train	1.8737 * e <sup>-5</sup>	0.98587	0.00305	0.00433	
		Test	2.3435 * e <sup>-5</sup>	0.97054	0.00388	0.00484	
	LS-SVM	Train	2.0793 * e <sup>-6</sup>	0.99843	0.00108	0.00144	
		Test	1.0853 * e <sup>-6</sup>	0.99864	0.00092	0.00104	
	Viscosity	BP	Train	0.00202	0.88871	0.03186	0.04496
			Test	0.00130	0.92447	0.02721	0.03600
RBF-BP		Train	6.8713 * e <sup>-5</sup>	0.99622	0.00691	0.00829	
		Test	2.9337 * e <sup>-5</sup>	0.99829	0.00415	0.00542	
RB-SVM		Train	0.00088	0.95153	0.02544	0.02967	
		Test	0.00103	0.94011	0.02627	0.03206	
LS-SVM		Train	5.1781 * e <sup>-6</sup>	0.99972	0.00182	0.00228	
		Test	8.1397 * e <sup>-6</sup>	0.99952	0.00230	0.00285	

It can be concluded from this that the BP artificial neural network is unsuitable for small data volume TiO<sub>2</sub>/water nanofluid compared to the support vector machine. When predicting two sets of data with the RB-SVM model, the parameters fluctuate wildly, which indicates that its predictive classification of two sets of data will be biased due to fuzzy classifications of some data, resulting in poor accuracy as a result. The LS-SVM model shows better prediction accuracy when predicting both data sets, but the LS-SVM model has higher accuracy in comparison. Therefore, LS-SVM is the most accurate neural network model for predicting the thermal conductivity of TiO<sub>2</sub> nanofluid with a small amount of data. In contrast, the other models are less accurate in comparison.

### 4.3 Accuracy Analysis of the Optimal Model

Figs. 11 and 12 compare the laboratory and machine learning predictions to understand better whether the predicted values are similar to the experimental values. The model accuracy is high when the prediction points are on or near the contour. The LS-SVM model has most of its points near the contour, as shown in the figure. The proposed machine learning algorithm has the highest accuracy among the selected models.

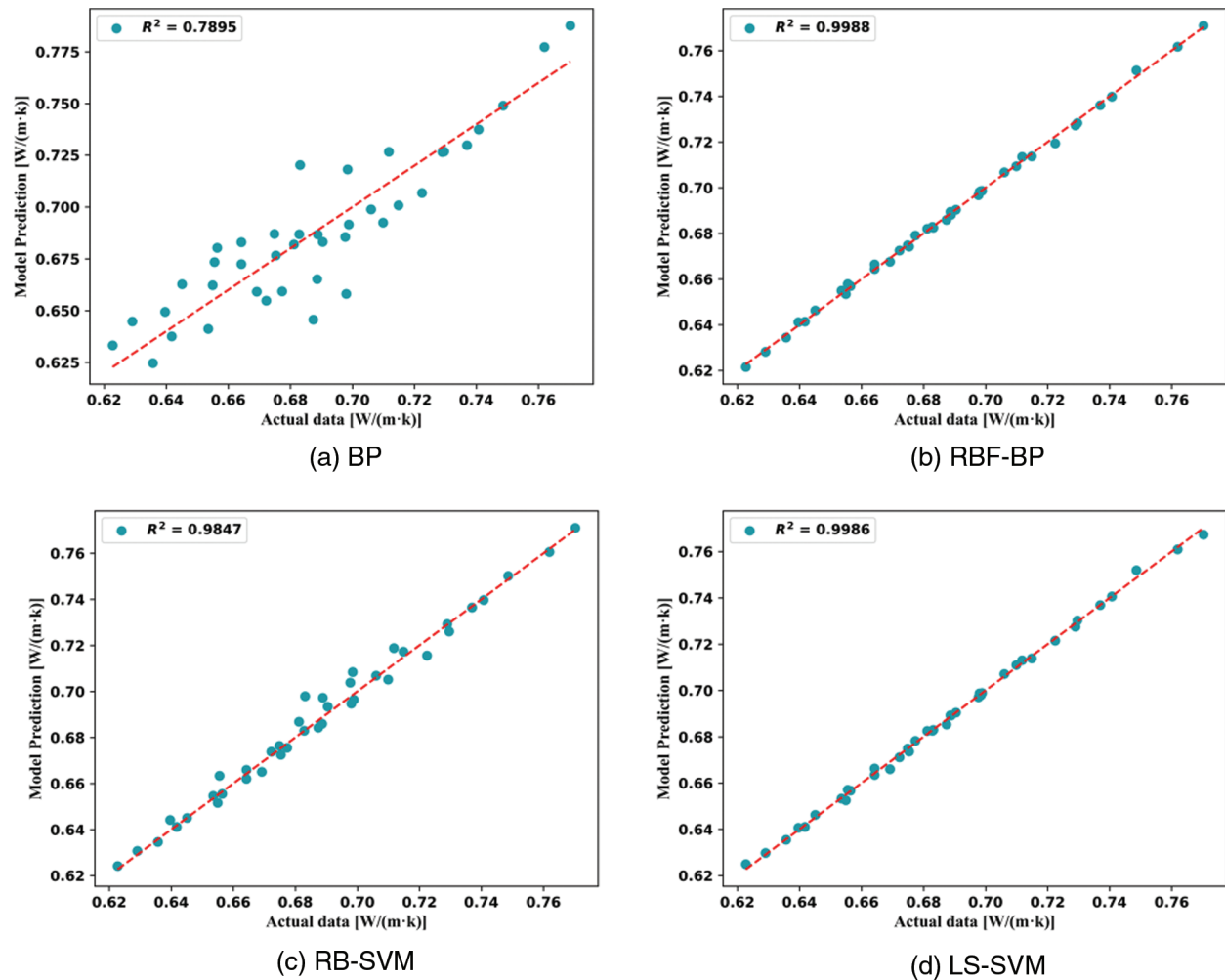


**Figure 11:** Comparison of actual data on thermal conductivity of  $\text{TiO}_2/\text{water}$  nanofluid with machine learning

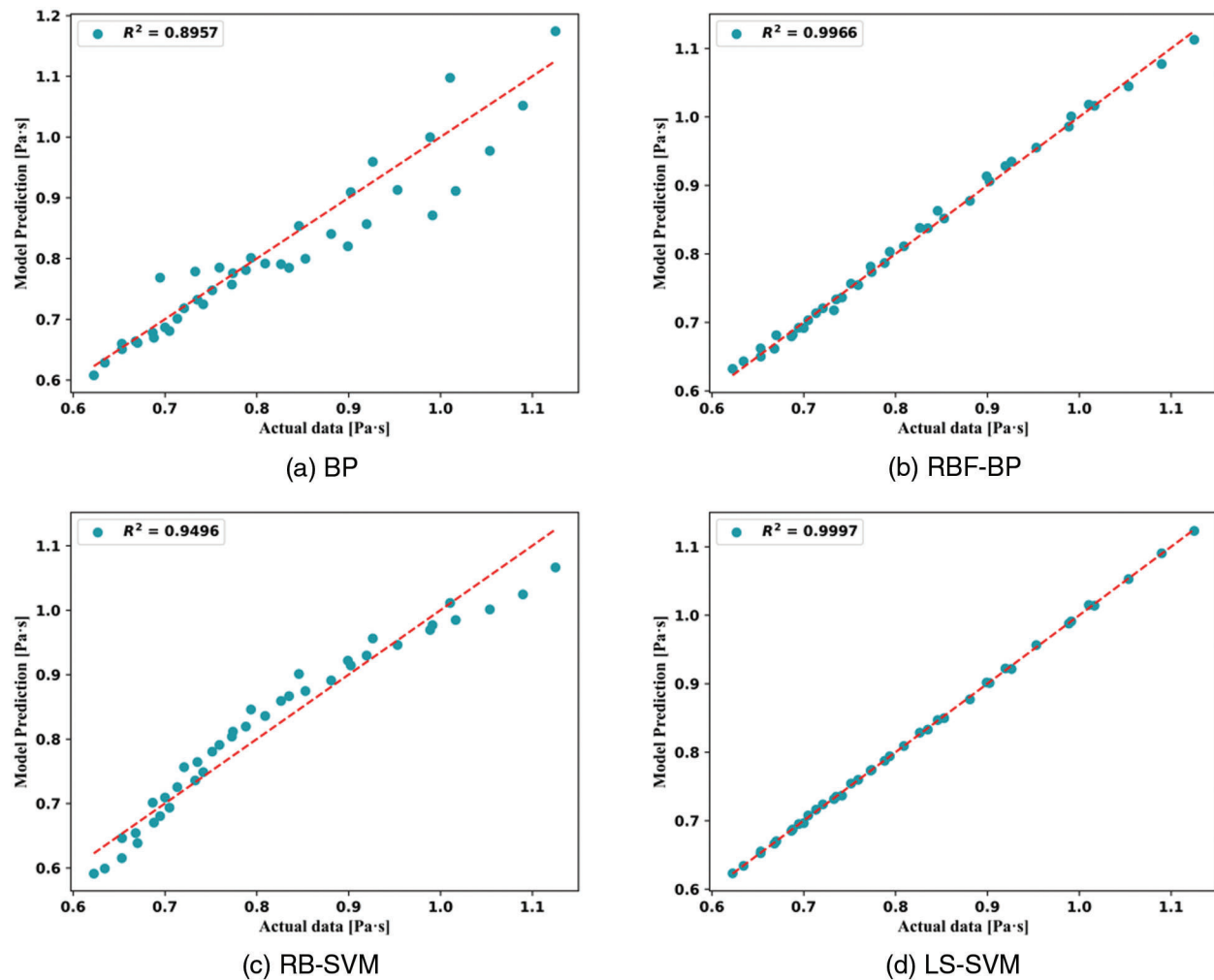


**Figure 12:** Comparison of actual  $\text{TiO}_2$ /water nanofluid viscosity data with machine learning

## 5 Conclusion

Nanofluids are famous heat and mass transfer materials in various fields at this stage. Thermal conductivity and viscosity are the most important thermophysical properties, and nanofluids operating temperature, volume fraction, particle morphology, and particle size directly affect their thermal conductivity and viscosity. In this study, focusing on experimental data, the effects of  $\text{TiO}_2$  concentration and temperature on nanofluids' thermal conductivity and viscosity were investigated by curve fitting, artificial neural network, and support vector machine methods. We propose a simple bivariate correlation using curve fitting to show the relationship between the parameters. Then, four machine learning models are selected to predict thermal conductivity and viscosity, with temperature and concentration as input variables. Based on the  $\text{MSE} = 1.82 \times 10^{-6}$  and  $\text{MSE} = 0.4942$  [64,65] models in the literature, it can show that the four models have reasonable predictions after normalization and grid search CV. In addition, the LS-SVM model shows high accuracy through four evaluation indexes without over-fitting or under-fitting. Curve fitting and neural networks are both good prediction tools. However, the LS-SVM model is more accurate and can better predict nanofluids' thermal conductivity and viscosity.

The results show that a better and more accurate model can better predict the model. For future research, it is necessary to examine the universal application of the model. This includes the influence of different input conditions on the model as well as the possibility that the model can still be applied after replacing the nanofluid. It is also necessary to develop a database of the model with high accuracy and strong applicability. As a result, this area requires further research.

**Funding Statement:** This research is financially supported by the National Natural Science Foundation of China (Nos. 51966005, 51866003) and Yunnan Basic Research Program Project (2019FB071).

**Conflicts of Interest:** The authors declare that they have no conflicts of interest to report regarding the present study.

## References

1. Cao, Y., Doustgani, A., Salehi, A., Nemati, M., Ghasemi, A. et al. (2020). The economic evaluation of establishing a plant for producing biodiesel from edible oil wastes in oil-rich countries: Case study Iran. *Energy*, 213, 118760. <https://doi.org/10.1016/j.energy.2020.118760>
2. Toghraie, D., Sina, N., Jolfaei, N. A., Hajian, M., Afrand, M. (2019). Designing an artificial neural network (ANN) to predict the viscosity of silver/ethylene glycol nanofluid at different temperatures and volume fraction of nanoparticles. *Physica A: Statistical Mechanics and its Applications*, 534, 122142. <https://doi.org/10.1016/j.physa.2019.122142>
3. Toghraie, D., Aghahadi, M. H., Sina, N., Soltani, F. (2020). Application of artificial neural networks (ANNs) for predicting the viscosity of tungsten oxide (WO<sub>3</sub>)-MWCNTs/engine oil hybrid nanofluid. *International Journal of Thermophysics*, 41(12), 1–17. <https://doi.org/10.1007/s10765-020-02749-x>
4. Karim, S. H. T., Tofiq, T. A., Shariati, M., Rad, H. N., Ghasemi, A. (2021). 4E analyses and multi-objective optimization of a solar-based combined cooling, heating, and power system for residential applications. *Energy Reports*, 7, 1780–1797. <https://doi.org/10.1016/j.egy.2021.03.020>
5. Ali, M. K. A., Xianjun, H., Abdelkareem, M. A., Gulzar, M., Elsheikh, A. H. (2018). Novel approach of the graphene nanolubricant for energy saving via anti-friction/wear in automobile engines. *Tribology International*, 124, 209–229. <https://doi.org/10.1016/j.triboint.2018.04.004>
6. Ali, M. K. A., Hou, X. J., Abdelkareem, M. A., Elsheikh, A. H. (2019). Role of nanolubricants formulated in improving vehicle engines performance. *IOP Conference Series: Materials Science and Engineering*, 563(2), 022015. <https://doi.org/10.1088/1757-899X/563/2/022015>
7. Essa, F. A., Yu, J., Elsheikh, A. H., Tawfik, M. M. (2019). A new M50 matrix composite sintered with a hybrid Sns/Zno nanoscale solid lubricants: An experimental investigation. *Materials Research Express*, 6(11), 116523. <https://doi.org/10.1088/2053-1591/ab4675>
8. Reddy, P. S., Chamkha, A. J. (2016). Influence of size, shape, type of nanoparticles, type and temperature of the base fluid on natural convection MHD of nanofluids. *Alexandria Engineering Journal*, 55(1), 331–341. <https://doi.org/10.1016/j.aej.2016.01.027>
9. Zayed, M. E., Sharshir, S. W., Shaibo, J., Hammad, F. A., Ali, M. K. A. et al. (2019). Applications of nanofluids in direct absorption solar collectors. In: *Nanofluids and their engineering applications*, pp. 405–429. CRC Press.
10. Elsheikh, A. H., Sharshir, S. W., Mostafa, M. E., Essa, F. A., Ali, M. K. A. (2018). Applications of nanofluids in solar energy: A review of recent advances. *Renewable and Sustainable Energy Reviews*, 82, 3483–3502. <https://doi.org/10.1016/j.rser.2017.10.108>
11. Huminic, A., Huminic, G., Fleaca, C., Dumitrache, F., Morjan, I. (2015). Thermal conductivity, viscosity and surface tension of nanofluids based on FeC nanoparticles. *Powder Technology*, 284, 78–84. <https://doi.org/10.1016/j.powtec.2015.06.040>
12. Sharshir, S. W., Peng, G., Elsheikh, A. H., Edreis, E. M., Eltawil, M. A. et al. (2018). Energy and exergy analysis of solar stills with micro/nano particles: A comparative study. *Energy Conversion and Management*, 177, 363–375. <https://doi.org/10.1016/j.enconman.2018.09.074>

13. Sharshir, S. W., Kandeal, A. W., Ismail, M., Abdelaziz, G. B., Kabeel, A. E. et al. (2019). Augmentation of a pyramid solar still performance using evacuated tubes and nanofluid: Experimental approach. *Applied Thermal Engineering*, 160, 113997. <https://doi.org/10.1016/j.applthermaleng.2019.113997>
14. Sharshir, S. W., Peng, G., Wu, L., Yang, N., Essa, F. A. et al. (2017). Enhancing the solar still performance using nanofluids and glass cover cooling: Experimental study. *Applied Thermal Engineering*, 113, 684–693. <https://doi.org/10.1016/j.applthermaleng.2016.11.085>
15. Sundar, L. S., Ramana, E. V., Graça, M. P. F., Singh, M. K., Sousa, A. C. (2016). Nanodiamond-Fe<sub>3</sub>O<sub>4</sub> nanofluids: Preparation and measurement of viscosity, electrical and thermal conductivities. *International Communications in Heat and Mass Transfer*, 73, 62–74. <https://doi.org/10.1016/j.icheatmasstransfer.2016.02.013>
16. Agarwal, R., Verma, K., Agrawal, N. K., Singh, R. (2017). Sensitivity of thermal conductivity for Al<sub>2</sub>O<sub>3</sub> nanofluids. *Experimental Thermal and Fluid Science*, 80, 19–26. <https://doi.org/10.1016/j.expthermflusci.2016.08.007>
17. Kim, H. J., Lee, S. H., Lee, J. H., Jang, S. P. (2015). Effect of particle shape on suspension stability and thermal conductivities of water-based bohemite alumina nanofluids. *Energy*, 90, 1290–1297. <https://doi.org/10.1016/j.energy.2015.06.084>
18. Sarafraz, M. M., Nikkhah, V., Madani, S. A., Jafarian, M., Hormozi, F. (2017). Low-frequency vibration for fouling mitigation and intensification of thermal performance of a plate heat exchanger working with CuO/water nanofluid. *Applied Thermal Engineering*, 121, 388–399. <https://doi.org/10.1016/j.applthermaleng.2017.04.083>
19. Sheikhabahi, M., Esfahany, M. N., Etesami, N. (2012). Experimental investigation of pool boiling of Fe<sub>3</sub>O<sub>4</sub>/ethylene glycol–water nanofluid in electric field. *International Journal of Thermal Sciences*, 62, 149–153. <https://doi.org/10.1016/j.ijthermalsci.2011.10.004>
20. Salari, E., Peyghambarzadeh, M., Sarafraz, M., Hormozi, F. (2016). Boiling heat transfer of alumina nano-fluids: Role of nanoparticle deposition on the boiling heat transfer coefficient. *Periodica Polytechnica Chemical Engineering*, 60(4), 252–258.
21. Nakhjavani, M., Nikkhah, V., Sarafraz, M. M., Shoja, S., Sarafraz, M. (2017). Green synthesis of silver nanoparticles using green tea leaves: Experimental study on the morphological, rheological and antibacterial behaviour. *Heat and Mass Transfer*, 53(10), 3201–3209. <https://doi.org/10.1007/s00231-017-2065-9>
22. Nikkhah, V., Sarafraz, M. M., Hormozi, F. (2015). Application of spherical copper oxide (II) water nano-fluid as a potential coolant in a boiling annular heat exchanger. *Chemical and Biochemical Engineering Quarterly*, 29(3), 405–415. <https://doi.org/10.15255/CABEQ.2014.2069>
23. Kamalgharibi, M., Hormozi, F., Zamzamian, S. A. H., Sarafraz, M. M. (2016). Experimental studies on the stability of CuO nanoparticles dispersed in different base fluids: Influence of stirring, sonication and surface-active agents. *Heat and Mass Transfer*, 52(1), 55–62. <https://doi.org/10.1007/s00231-015-1618-z>
24. Said, Z., Sharma, P., Sundar, L. S., Afzal, A., Li, C. (2021). Synthesis, stability, thermophysical properties and AI approach for predictive modelling of Fe<sub>3</sub>O<sub>4</sub> coated MWCNT hybrid nanofluids. *Journal of Molecular Liquids*, 340, 117291. <https://doi.org/10.1016/j.molliq.2021.117291>
25. Sharma, P., Sharma, A. K. (2021). Application of response surface methodology for optimization of fuel injection parameters of a dual fuel engine fuelled with producer gas-biodiesel blends. *Energy Sources, Part A: Recovery, Utilization, and Environmental Effects*, 1–18. <https://doi.org/10.1080/15567036.2021.1892883>
26. Sharma, P. (2022). Prediction-optimization of the effects of di-tert butyl peroxide-biodiesel blends on engine performance and emissions using multi-objective response surface methodology. *Journal of Energy Resources Technology*, 144(7). <https://doi.org/10.1115/1.4052237>
27. Sharma, P. (2020). Gene expression programming-based model prediction of performance and emission characteristics of a diesel engine fueled with linseed oil biodiesel/diesel blends: An artificial intelligence approach. *Energy Sources, Part A: Recovery, Utilization, and Environmental Effects*, 1–15. <https://doi.org/10.1080/15567036.2020.1829204>

28. Sharma, P. (2021). Artificial intelligence-based model prediction of biodiesel-fueled engine performance and emission characteristics: A comparative evaluation of gene expression programming and artificial neural network. *Heat Transfer*, 50(6), 5563–5587. <https://doi.org/10.1002/hjt.22138>
29. Wang, J., Zhai, Y., Yao, P., Ma, M., Wang, H. (2020). Established prediction models of thermal conductivity of hybrid nanofluids based on artificial neural network (ANN) models in waste heat system. *International Communications in Heat and Mass Transfer*, 110, 104444. <https://doi.org/10.1016/j.icheatmasstransfer.2019.104444>
30. Said, Z., Sundar, L. S., Rezk, H., Nassef, A. M., Ali, H. M. et al. (2021). Optimizing density, dynamic viscosity, thermal conductivity and specific heat of a hybrid nanofluid obtained experimentally via ANFIS-based model and modern optimization. *Journal of Molecular Liquids*, 321, 114287. <https://doi.org/10.1016/j.molliq.2020.114287>
31. Jamei, M., Ahmadianfar, I., Olumegbon, I. A., Asadi, A., Karbasi, M. et al. (2021). On the specific heat capacity estimation of metal oxide-based nanofluid for energy perspective—A comprehensive assessment of data analysis techniques. *International Communications in Heat and Mass Transfer*, 123, 105217. <https://doi.org/10.1016/j.icheatmasstransfer.2021.105217>
32. Alnaqi, A. A., Alsarraf, J., Al-Rashed, A. A. (2021). Using response surface methodology and artificial neural network to examine the rheological behavior of tungsten trioxide/ethylene glycol nanofluid under various sonication times. *Journal of Molecular Liquids*, 337, 116022. <https://doi.org/10.1016/j.molliq.2021.116022>
33. Ilyas, S. U., Ridha, S., Sardar, S., Estellé, P., Kumar, A. et al. (2021). Rheological behavior of stabilized diamond-graphene nanoplatelets hybrid nanosuspensions in mineral oil. *Journal of Molecular Liquids*, 328, 115509. <https://doi.org/10.1016/j.molliq.2021.115509>
34. Li, X., Wang, H., Luo, B. (2021). The thermophysical properties and enhanced heat transfer performance of SiC-MWCNTs hybrid nanofluids for car radiator system. *Colloids and Surfaces A: Physicochemical and Engineering Aspects*, 612, 125968. <https://doi.org/10.1016/j.colsurfa.2020.125968>
35. Akhgar, A., Toghraie, D., Sina, N., Afrand, M. (2019). Developing dissimilar artificial neural networks (ANNs) to prediction the thermal conductivity of MWCNT-TiO<sub>2</sub>/Water-ethylene glycol hybrid nanofluid. *Powder Technology*, 355, 602–610. <https://doi.org/10.1016/j.powtec.2019.07.086>
36. Rostami, S., Toghraie, D., Shabani, B., Sina, N., Barnoon, P. (2021). Measurement of the thermal conductivity of MWCNT-CuO/water hybrid nanofluid using artificial neural networks (ANNs). *Journal of Thermal Analysis and Calorimetry*, 143(2), 1097–1105. <https://doi.org/10.1007/s10973-020-09458-5>
37. Li, X., Zeng, G., Lei, X. (2020). The stability, optical properties and solar-thermal conversion performance of SiC-MWCNTs hybrid nanofluids for the direct absorption solar collector (DASC) application. *Solar Energy Materials and Solar Cells*, 206, 110323. <https://doi.org/10.1016/j.solmat.2019.110323>
38. Ahammed, N., Asirvatham, L. G., Wongwises, S. (2016). Effect of volume concentration and temperature on viscosity and surface tension of graphene–water nanofluid for heat transfer applications. *Journal of Thermal Analysis and Calorimetry*, 123(2), 1399–1409. <https://doi.org/10.1007/s10973-015-5034-x>
39. Harandi, S. S., Karimipour, A., Afrand, M., Akbari, M., D’Orazio, A. (2016). An experimental study on thermal conductivity of F-MWCNTs–Fe<sub>3</sub>O<sub>4</sub>/EG hybrid nanofluid: Effects of temperature and concentration. *International Communications in Heat and Mass Transfer*, 76, 171–177. <https://doi.org/10.1016/j.icheatmasstransfer.2016.05.029>
40. Toghraie, D., Chaharsoghi, V. A., Afrand, M. (2016). Measurement of thermal conductivity of ZnO–TiO<sub>2</sub>/EG hybrid nanofluid. *Journal of Thermal Analysis and Calorimetry*, 125(1), 527–535. <https://doi.org/10.1007/s10973-016-5436-4>
41. Soylu, S. K., Acar, Z. Y., Asiltürk, M., Atmaca, İ. (2022). Effects of doping on the thermophysical properties of Ag and Cu doped TiO<sub>2</sub> nanoparticles and their nanofluids. *Journal of Molecular Liquids*, 368, 120615.
42. Alirezaie, A., Saedodin, S., Esfe, M. H., Rostamian, S. H. (2017). Investigation of rheological behavior of MWCNT (COOH-functionalized)/MgO-engine oil hybrid nanofluids and modelling the results with artificial neural networks. *Journal of Molecular Liquids*, 241, 173–181.
43. Sharma, P., Said, Z., Kumar, A., Nizetic, S., Pandey, A. et al. (2022). Recent advances in machine learning research for nanofluid-based heat transfer in renewable energy system. *Energy & Fuels*, 36(13), 6626–6658.

44. Esfahani, N. N., Toghraie, D., Afrand, M. (2018). A new correlation for predicting the thermal conductivity of ZnO–Ag (50%–50%)/water hybrid nanofluid: An experimental study. *Powder Technology*, 323, 367–373.
45. Said, Z., Cakmak, N. K., Sharma, P., Sundar, L. S., Inayat, A. et al. (2022). Synthesis, stability, density, viscosity of ethylene glycol-based ternary hybrid nanofluids: Experimental investigations and model-prediction using modern machine learning techniques. *Powder Technology*, 400, 117190.
46. Sharma, P., Said, Z., Memon, S., Elavarasan, R. M., Khalid, M. et al. (2022). Comparative evaluation of AI-based intelligent GEP and ANFIS models in prediction of thermophysical properties of Fe<sub>3</sub>O<sub>4</sub>-coated MWCNT hybrid nanofluids for potential application in energy systems. *International Journal of Energy Research*, 46(13), 19242–19257.
47. Ariana, M. A., Vaferi, B., Karimi, G. (2015). Prediction of thermal conductivity of alumina water-based nanofluids by artificial neural networks. *Powder Technology*, 278, 1–10.
48. Masoumi, N., Sohrabi, N., Behzadmehr, A. (2009). A new model for calculating the effective viscosity of nanofluids. *Journal of Physics D: Applied Physics*, 42(5), 055501.
49. Kanti, P. K., Sharma, K. V., HN, A. R., Karbasi, M., Said, Z. (2022). Experimental investigation of synthesized Al<sub>2</sub>O<sub>3</sub> ionanofluid's energy storage properties: Model-prediction using gene expression programming. *Journal of Energy Storage*, 55, 105718.
50. Kanti, P., Sharma, K. V., Yashawantha, K. M., Dmk, S. (2021). Experimental determination for viscosity of fly ash nanofluid and fly ash-Cu hybrid nanofluid: Prediction and optimization using artificial intelligent techniques. *Energy Sources, Part A: Recovery, Utilization, and Environmental Effects*, 1–20.
51. Kanti, P. K., Sharma, K. V., Said, Z., Jamei, M., Yashawantha, K. M. (2022). Experimental investigation on thermal conductivity of fly ash nanofluid and fly ash-Cu hybrid nanofluid: Prediction and optimization via ANN and MGGP model. *Particulate Science and Technology*, 40(2), 182–195.
52. Kanti, P., Sharma, K. V., Jamei, M., Kumar, H. P. (2021). Thermal performance of hybrid fly ash and copper nanofluid in various mixture ratios: Experimental investigation and application of a modern ensemble machine learning approach. *International Communications in Heat and Mass Transfer*, 129, 105731.
53. Kanti, P., Sharma, K. V., Yashawantha, K. M., Jamei, M., Said, Z. (2022). Properties of water-based fly ash-copper hybrid nanofluid for solar energy applications: Application of RBF model. *Solar Energy Materials and Solar Cells*, 234, 111423.
54. Hemmat Esfe, M., Rostamian, H., Toghraie, D., Yan, W. M. (2016). Using artificial neural network to predict thermal conductivity of ethylene glycol with alumina nanoparticle. *Journal of Thermal Analysis and Calorimetry*, 126(2), 643–648.
55. He, W., Ruhani, B., Toghraie, D., Izadpanahi, N., Esfahani, N. N. et al. (2020). Using of artificial neural networks (ANNs) to predict the thermal conductivity of zinc oxide–silver (50%–50%)/water hybrid newtonian nanofluid. *International Communications in Heat and Mass Transfer*, 116, 104645.
56. Rostami, S., Toghraie, D., Esfahani, M. A., Hekmatifar, M., Sina, N. (2021). Predict the thermal conductivity of SiO<sub>2</sub>/water–ethylene glycol (50:50) hybrid nanofluid using artificial neural network. *Journal of Thermal Analysis and Calorimetry*, 143(2), 1119–1128.
57. Tian, S., Arshad, N. I., Toghraie, D., Eftekhari, S. A., Hekmatifar, M. (2021). Using perceptron feed-forward artificial neural network (ANN) for predicting the thermal conductivity of graphene oxide-Al<sub>2</sub>O<sub>3</sub>/water-ethylene glycol hybrid nanofluid. *Case Studies in Thermal Engineering*, 26, 101055.
58. Zhang, H., Qing, S., Xu, J., Zhang, X., Zhang, A. (2022). Stability and thermal conductivity of TiO<sub>2</sub>/water nanofluids: A comparison of the effects of surfactants and surface modification. *Colloids and Surfaces A: Physicochemical and Engineering Aspects*, 641, 128492.
59. Sonawane, S. S., Khedkar, R. S., Wasewar, K. L. (2015). Effect of sonication time on enhancement of effective thermal conductivity of nano TiO<sub>2</sub>–water, ethylene glycol, and paraffin oil nanofluids and models comparisons. *Journal of Experimental Nanoscience*, 10(4), 310–322.
60. LeCun, Y., Touresky, D., Hinton, G., Sejnowski, T. (1988). A theoretical framework for back-propagation. *Proceedings of the 1988 Connectionist Models Summer School*, 1, 21–28.

61. Hearst, M. A., Dumais, S. T., Osuna, E., Platt, J., Scholkopf, B. (1998). Support vector machines. *IEEE Intelligent Systems and their Applications*, 13(4), 18–28. <https://doi.org/10.1109/5254.708428>
62. Ahmadi, M. A., Ebadi, M., Marghmaleki, P. S., Fouladi, M. M. (2014). Evolving predictive model to determine condensate-to-gas ratio in retrograded condensate gas reservoirs. *Fuel*, 124, 241–257. <https://doi.org/10.1016/j.fuel.2014.01.073>
63. Fazeli, H., Soleimani, R., Ahmadi, M. A., Badrmezhad, R., Mohammadi, A. H. (2013). Experimental study and modeling of ultrafiltration of refinery effluents using a hybrid intelligent approach. *Energy & Fuels*, 27(6), 3523–3537. <https://doi.org/10.1021/ef400179b>
64. Maleki, A., Haghighi, A., Mahariq, I. (2021). Machine learning-based approaches for modeling thermophysical properties of hybrid nanofluids: A comprehensive review. *Journal of Molecular Liquids*, 322, 114843. <https://doi.org/10.1016/j.molliq.2020.114843>
65. Gholami, E., Vaferi, B., Ariana, M. A. (2018). Prediction of viscosity of several alumina-based nanofluids using various artificial intelligence paradigms-comparison with experimental data and empirical correlations. *Powder Technology*, 323, 495–506. <https://doi.org/10.1016/j.powtec.2017.10.038>